

Hybrid Transformer Model for Transient Simulation—Part I: Development and Parameters

Bruce A. Mork, *Member, IEEE*, Francisco Gonzalez, Dmitry Ishchenko, *Member, IEEE*,
Don L. Stuehm, *Member, IEEE*, and Joydeep Mitra, *Senior Member, IEEE*

Abstract—A new topologically correct hybrid transformer model is developed for low and midfrequency transient simulations. Power transformers have a conceptually simple design, but behaviors can be very complex. The selection of the most suitable representation for a given behavior depends on the type of transformer to be simulated, the frequency range, and other factors, such as the internal design of the transformer and available parameters or design data. Here, a modular model suitable for frequencies up to 3–5 kHz is developed, utilizing a duality-based lumped-parameter saturable core, matrix descriptions of leakage and capacitive effects, and frequency-dependent coil resistance. Implementation and testing of this model was done for 15-kVA 208 Δ -120Y 3-legged and 150-kVA 12,470Y-208Y 5-legged transformers. The basis and development of the model is presented, along with a discussion of necessary parameters and the approaches for obtaining them.

Index Terms—Duality, Electromagnetic Transients Program (EMTP), transformer models, transient simulations.

I. INTRODUCTION

GR^{EAT} advancements have been made in transient simulation software over the last 30 years. Traditional transient network analyzer (TNA) systems have essentially been replaced by computer simulation. However, improvements must still be made in many of the individual component models used in transient simulation packages. Transformer models are one of the components most in need of advancement [1]–[6]. Although power transformers are a conceptually simple design, their representation can be very complex due to different core and coil configurations, and magnetic saturation, which can markedly affect transient behavior.

It is difficult to apply one acceptable representation throughout the complete range of frequencies for all possible transient phenomena in a power system. One or several models valid for a specific frequency range might be used. According to [7], frequency ranges can be classified in four

Manuscript received January 10, 2006; revised May 10, 2006. This work was supported in part by Bonneville Power Administration, in part by the U.S. Department of Energy, in part by the Spanish Secretary of State of Education and Universities, in part by the European Social Fund, in part by the Fulbright, in part by the Norwegian Research Council, and the Norwegian Electric Power Research Institute. Paper no. TPWRD-00760-2005.

B. A. Mork, F. Gonzalez, and D. Ishchenko are with the Department of Electrical Engineering, Michigan Technological University, Houghton, MI 49931 USA.

D. L. Stuehm is with the Department of Electrical Engineering, North Dakota State University, Fargo, ND 58105 USA.

J. Mitra is with the Department of Electrical Engineering, New Mexico State University, Las Cruces, NM 88003 USA.

Digital Object Identifier 10.1109/TPWRD.2006.883000

groups with some overlapping between them. See Table I for more detail.

The work presented here makes advancements on the traditional transformer models in Electromagnetic Transients Program (EMTP) [8], [9]. The focus is on improvement of low and midfrequency model topology and correctness, and developing more specific modeling details. A hybrid model is proposed, using the strength of the inverse inductance matrix $[A]$ for leakage representation [8], [9], the principle of duality for topologically correct core representation [1]–[6], and incorporating capacitive effects and the frequency dependency of coil resistances. This model is now available in Alternative Transients Program (ATP)/EMTP [10] with details available in the public domain.

II. EXISTING TRANSFORMER MODELS

The transformer models now in use have different levels of detail depending on the application. None of them are able to simulate all transient phenomena for all frequency ranges.

A simplified linear representation of single- and three-phase transformers can be implemented in EMTP in the form of branch impedance or admittance matrices using the BCTRAN routine [8], [9]. However, this approach cannot include multi-limb topology or nonlinear effects of the iron core. For transient analysis of ferroresonance, inrush currents, and other nonlinear behaviors, it is necessary to consider saturation effects. Although the excitation branch may be externally attached to the model in the form of nonlinear elements (similar to Fig. 1), such an externally attached core is not necessarily topologically correct.

Saturation effects might also be included in EMTP by attaching a nonlinear inductor at the fictitious star point of a three-winding star-circuit model. However, this model also has some limitations. The most important are: possible numerical instability, which can be observed for the three-winding case, but can be solved by some modifications of the traditional model as in [11]; limited usefulness for three-phase units; and connection of nonlinear magnetizing inductance to the star point which is not topologically correct [8], [9].

Detailed models incorporating core nonlinearities can be derived by using the principle of duality [1], [4]–[6]. In this case, models include the saturation effects for each individual limb of the core, leakage effects, and magnetic coupling. These models are based on the development of a lumped-parameter magnetic circuit representing the flux paths in the core and coils of a transformer, and the subsequent conversion of this magnetic circuit to an equivalent electric circuit using duality transformations.

TABLE I
MODELING OF POWER TRANSFORMERS

PARAMETER / EFFECT	LOW FREQUENCY TRANSIENTS	SLOW FRONT TRANSIENTS	FAST FRONT TRANSIENTS	VERY FAST TRANSIENTS
Short-circuit impedance	Very important	Very important	Important	Negligible
Saturation	Very important	Very important ¹⁾	Negligible	Negligible
Iron losses	Important ²⁾	Important	Negligible	Negligible
Eddy currents	Very important	Important	Negligible	Negligible
Capacitive coupling	Negligible	Important	Very important	Very important

1) Only for transformer energization phenomena, otherwise important.

2) Only for resonance phenomena.

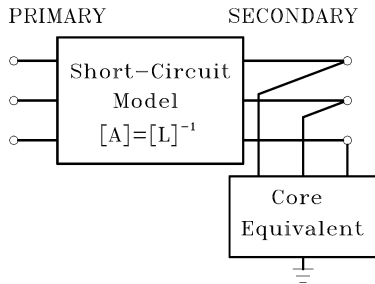


Fig. 1. Basic concept of combining inverse inductance matrix with externally attached core for two-winding transformer.

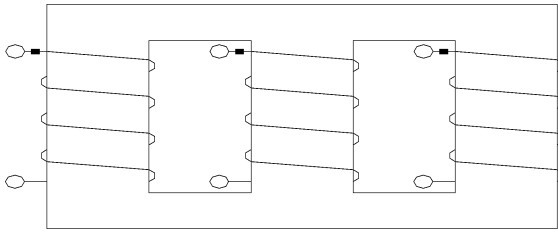


Fig. 2. Three-legged stacked core transformer. For simplicity, only one set of windings is shown.

III. NEW APPROACH: HYBRID MODEL

Based on the discussion of the previous section and as reported in [12], it seems practical to develop a combined or “hybrid” model based on improvements to the general idea of Fig. 1.

The combination of components and improvements are

- to use the $[A]$ matrix for complete leakage inductance representation and adding core-coil couplings;
- to use a nonlinear duality-based topologically correct representation of the core;
- to utilize frequency-dependent winding resistances;
- to include capacitive effects, externally attached to the bushing terminals of the model.

A. Duality-Based Core Representation

A three-legged stacked core wye–delta transformer is used here as an example [12]. Figs. 2 and 3 show the physical structure and the corresponding lumped magnetic circuit. The R 's in Fig. 3 denote magnetic reluctances. The complete derivation of this model following the principle of duality is given in [12] and [13].

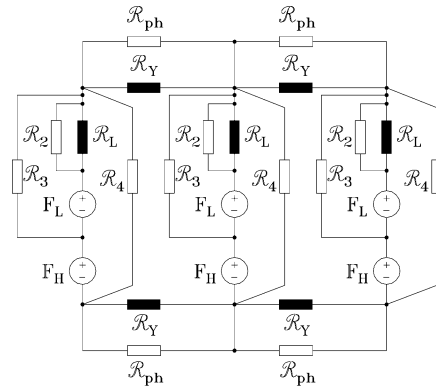


Fig. 3. Magnetic circuit. Reluctances represent flux paths. Shaded R s are magnetic core and limbs, unshaded R s are leakage flux paths.

The basic process for creating an equivalent electrical circuit using this technique is summarized as follows [4]. First, flux paths are assumed and then the lumped-parameter magnetic circuit is drawn. The magnetic circuit is transformed into an electric model using duality transformation. The final step is to replace current sources with ideal coupling transformers, then add winding resistances, core losses, and capacitive coupling effects. One disadvantage of the duality-based short-circuit model is the lack of a detailed leakage representation, but that can be overcome by using the $[A]$ matrix for leakage while retaining the topologically correct duality-derived core model.

In Fig. 3, R_L represents the flux path through the legs, R_Y corresponds to the flux path through the yoke; R_2 represents leakage path between the legs and the innermost winding; there is a leakage path between the legs and the space between the two windings (R_3), and between the legs and outside windings (R_4); finally, R_{ph} represents flux leakage path through air in parallel with the yokes.

The resulting equivalent circuit for this transformer is shown in Fig. 4. Four distinct functional parts are described as follows:

- 1) leakage representation;
- 2) topologically correct core representation;
- 3) winding resistances;
- 4) capacitive effects.

Fig. 5 shows the resulting hybrid transformer model: Two matrices representing the leakage and the capacitive effects, the frequency-dependent resistances described with a Foster circuit of

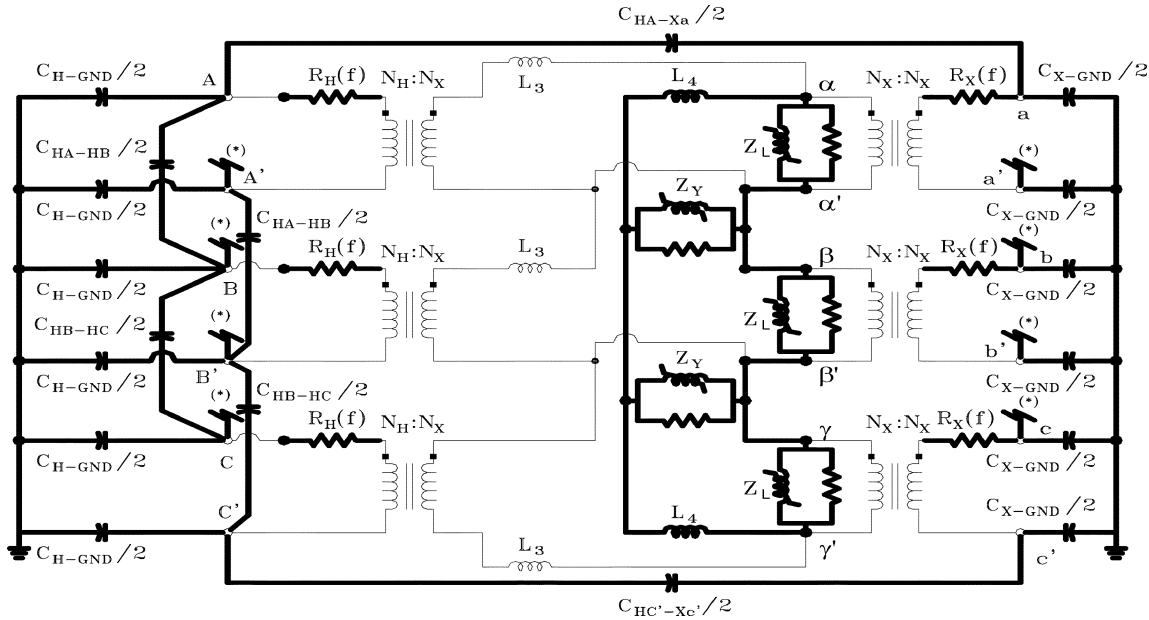


Fig. 4. Duality-based hybrid model. (*) connection point for coil-to-coil capacitances, only 2 of 6 are shown.

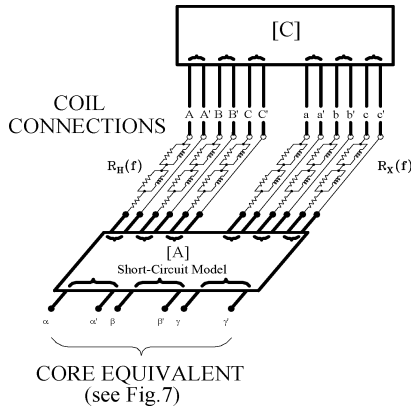


Fig. 5. [A] matrix-based leakage equivalent with capacitance overlay and frequency-dependent coil resistance. Core attaches to $N + 1$ th winding.

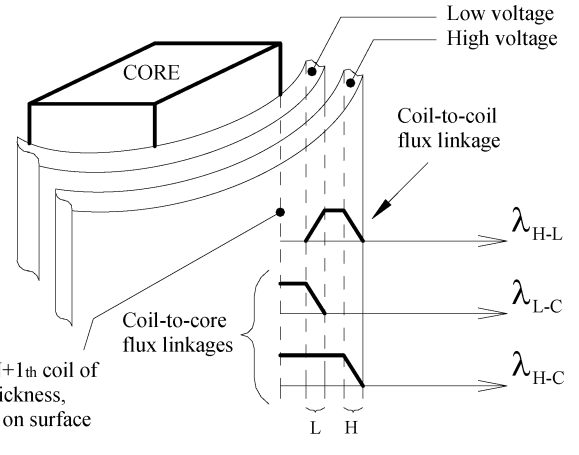


Fig. 6. Conceptual implementation of $N + 1$ th winding flux leakage model.

two cells, and the duality-based core attached to the fictitious $N + 1$ th winding. This is thus a modular representation of the detailed model of Fig. 4. This hybrid model combines the strengths of different approaches, creating a universal model that can be adapted to specific core and coil configurations. Note that the model is independent of coil connection as delta, wye, auto, and zig-zag connections are made by jumpering the external connections.

B. Leakage Inductance

Leakage inductance is due to flux linking one winding but not another. The flux that “leaks” typically passes through air or other nonmagnetic materials and may also find low-reluctance paths through the transformer tank and other metallic fittings. Referring to Fig. 6, the distribution of leakage flux depends on the geometric configuration of the coils. One leakage effect, important for detailed models but not considered (or measurable) in factory tests, is the flux linked by the innermost winding (L

in this case) but not flowing in the core. This can be conceptually dealt with by assuming a fictitious infinitely thin $N + 1$ th “coil” at the surface of the core leg (C). The related flux linkage is labeled as L-C.

Short-circuit reactance between high- and low-voltage windings X_{HL} can be obtained from factory test reports. It can also be calculated from transformer design information. A detailed derivation of leakage reactance between windings is given in [14]–[16]. The relationship for the leakage reactance in Fig. 6 is

$$X_{HL} = \frac{\omega\mu_0 N^2}{h} \cdot \left(\frac{L_{mt,H}b_H}{3} + \frac{L_{mt,L}b_L}{3} + L_{mt,2a_2} \right) \quad (1)$$

where a is the duct or insulation thickness between coils, b is the coil thickness, $L_{mt} = 2\pi r_{mt}$ (if a circular coil is assumed) where r_{mt} is the distance from the center of the core leg to the mean turn of the respective windings, f represents the frequency $\omega = 2\pi f$, μ_0 is the magnetic permeability of air, h is the height of the winding, and N is the number of turns of either the high-

or low-voltage winding depending on which side of the transformer the leakage is referred to. This derivation assumes linear flux distribution across the coil thickness. For each binary pair of coils, the magnetomotive force increases linearly across the inner winding, remains constant across the duct, then decreases linearly with radius through the outer winding. Analogous relationships exist for segmented and pancake coils.

Values of the reactances between the core and each winding can be estimated according to a proportionality factor K , times the short-circuit reactance between windings. If the reactance between the core and the low-voltage winding is assumed to be $X_{LC} \approx K \cdot X_{HL}$, then the reactance between the core and high-voltage winding can be estimated as

$$X_{HC} \approx X_{LC} + X_{HL} = K \cdot X_{HL} + X_{HL} = (K + 1) \cdot X_{HL}. \quad (2)$$

The methodology used to calculate $[A]$ matrix parameters is explained in [8] and [17]. The fictitious winding at the surface of the core (C) is assumed to have the same voltage as the innermost winding. One point of the core is grounded externally, being included as a reference for the $[A]$ matrix. The $[A]$ matrix is a full three-phase representation, with 3×3 submatrices representing the effects between three-phase sets of coils. The elements of each submatrix include the effects of both positive- and zero-sequence behaviors.

C. Coupling Transformers

In the duality-derived model, coupling transformers provide isolation between the core equivalent and the external part of the transformer model (Fig. 4). These ideal transformers have no impedances and simply provide the required turns ratios [8]. The effect of these transformers is taken into account inside the inverse inductance matrix $[A]$. Voltages and currents in the $N+1$ th winding are always referred to the voltage level of the innermost coil.

D. Nonlinear Core

The fictitious $N+1$ th winding of $[A]$ is used as an attachment point for the core equivalent, as shown in Fig. 7 for a 3-legged core.

The topologically correct nonlinear representation of the core is extracted from the duality model and attached to the α - β - γ terminals of the $N+1$ th winding.

Each limb (Z_L) and yoke (Z_Y) is represented by a core-loss resistance in parallel with a saturable inductance. The zero-sequence flux paths are represented by inductances L_4 (for a five-legged core, each L_4 becomes a saturable core section corresponding to the outer legs).

This simplistic R-L representation for each limb of the core in Fig. 7 is satisfactory in many cases, but a more detailed representation could be applied if warranted (see Fig. 8). The L_M representation [18], [19], is based on the reversible anhysteretic saturation curve [20]. The total core loss R_C present in the transformer core consists of: hysteresis losses R_H , eddy current losses R_E , and anomalous losses R_A . The capacitance C_W is the aggregate total of the turn-to-turn winding capacitances. However, a simpler representation is used in the hybrid model. C_W

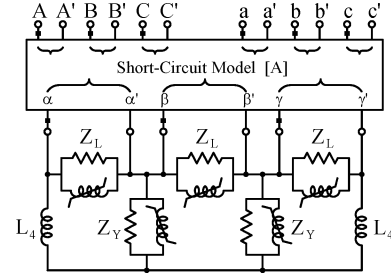


Fig. 7. Core attached to the $N + 1$ th winding.

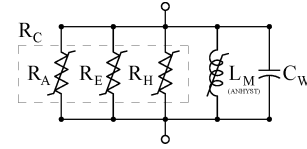


Fig. 8. More exact representation of each limb of core, based on anhysteretic saturation characteristic and detailed loss mechanisms.

is included in the capacitance matrix $[C]$, and R_A , R_E , and R_H are lumped in R_C , while L_M is from the normal curve (Figs. 5 and 7).

From available open-circuit test data, it is typically possible to know exciting current in % at 100% rated voltage and core losses in W at 100% rated voltage. In some cases, it is also possible to have this data at additional levels of rated voltage with 90% and 110% being the most common. A linear representation of the core is all that can directly be obtained if only data at 100% of the excitation voltage is available. For that reason, it is desirable to have several available levels from test reports in order to be able to build an accurate magnetizing curve [15].

If design data are available, the core equivalent can be determined based on the calculation of the λ - i magnetization curve for each limb of the core. Estimation of the magnetization curves is rather straightforward, since the material type is known, as well as the core dimensions (net cross-sectional areas and lengths) and number of turns of the windings. The material type defines the B-H curve, which is naturally the same for all the limbs of the transformer and can be approximated by the Frolich equation, which gives a smooth single-valued curve as a function of two parameters a and b

$$B = \frac{H}{a + b \cdot H}, \quad \mu = \frac{B}{H} = \frac{(1 - b \cdot B)}{a}. \quad (3)$$

The λ - i curves can be estimated by scaling the B-H curve according to the actual areas and lengths of the corresponding limbs. If dimensions of legs and yokes are unknown, the normalized ratios of core dimensions can be used. If the core dimension ratios are unknown, they can be assumed [15]. In these cases, typical ratios can be used without great error, since core dimension ratios vary within a small range according to standard design practice. The Frolich equation [21] is convenient to represent the core magnetization curve.

Test measurements can also serve as a source of data for estimating the λ - i magnetization curves for core limbs [4].

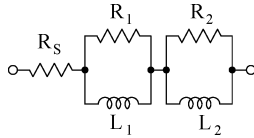


Fig. 9. Second-order series Foster circuit.

E. Frequency-Dependent Coil Resistance

Coil resistances vary depending on the frequency of the current flowing, mainly due to skin effect and proximity effect. The skin effect is caused by the nonuniform distribution of the magnetic field due to currents flowing within the conductor; as the frequency of the current increases, more current flows near the surface of the conductor, thus increasing the effective resistance. The proximity effect is due to external magnetic fields generated from current in surrounding conductors. In a transformer, a higher number of layers in the coil leads to significant resistance variation caused by this effect. The skin effect dominates the losses up to a certain frequency, above which the proximity effect also becomes apparent [22].

Data typically available from the factory test reports include power-frequency short-circuit losses and dc resistances, which can be used to obtain the parameters for coil resistances. A useful option, not common for factory test reports, is to measure frequency-dependent resistance over a range of frequencies. DC resistance measurements can also be very useful.

A second-order series Foster circuit seems to be the most straightforward robust representation (Fig. 9), as it is capable of fitting both skin and proximity effects [15]. When standard factory test reports are provided, assumptions on frequency-dependent behavior of winding resistances have to be made, based on transformer rated megavolt-amperes (MVA). Typical L/R ratios for transformers of different sizes as a function of frequency are provided in [8] and [23]. Based on that, typical ratios of the effective resistances for frequencies other than 60 Hz can be derived. The transformer leakage inductance is fairly constant through the range of frequencies.

In cases where design information is available, parameters can be obtained in two ways depending on whether dc resistances are known or frequency-dependent data are available. DC winding resistance depends on the material used and the coil arrangement, and can be calculated based on the physical design information. An approach that presents a more accurate consideration of proximity effect can be used [24]; otherwise, a fitting method can be implemented.

F. Capacitance

Capacitive effects may be significant and need to be included in the model, especially for large high-voltage transformers [15], [18]. The major coupling capacitances of the three-legged transformer example considered here are shown in Figs. 10 and 11. The general case with major capacitive effects is shown (Fig. 10). All capacitances have been divided into two equal parts to partially distribute the effects. Capacitances between the high- and low-voltage windings and the core C_{H-C} and C_{L-C} are included for each phase. Windings are separated by insulating material (oil and paper) effectively forming a

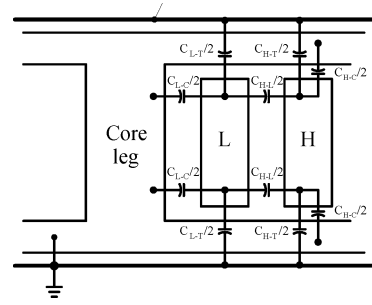


Fig. 10. Capacitances between core, windings, and tank.

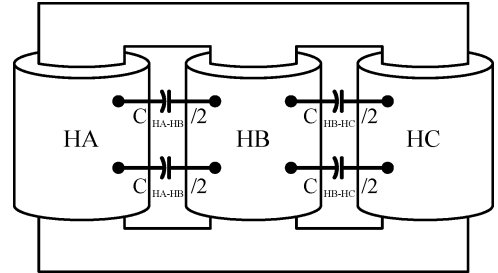


Fig. 11. Capacitances between phases of high-voltage windings.

parallel plate or coaxial capacitance C_{H-L} , which is connected from the outside of the low-voltage winding to the inside of the high-voltage winding. Other capacitances exist between the high- and low-voltage windings and the tank of the transformer C_{H-T} and C_{L-T} respectively; both capacitances include the effects of the bushings. There is no capacitance included between the core and the tank since both of them are connected to ground. Also, there are possible couplings between the high-voltage windings of phases A and B (HA and HB), and between phases B and C (HB and HC). The capacitance between HA and HC is negligible due to the large distance between the two and the presence of winding HB. Fig. 11 shows these capacitances in detail.

Manufacturers carry out capacitance measurements only if the purchase specification mandates. In this case, there are two basic kinds of measurements: Capacitance between windings, and capacitance between each winding and ground that include the capacitive effects between all grounded metallic surfaces (tank, core, etc.) and each winding.

If design information is available, the calculation of these various capacitances is possible. In core-type transformers with cylindrical configuration for the windings, winding-to-winding capacitance and winding-to-core capacitance C_{H-L} and C_{L-C} , respectively, can be calculated assuming that the windings can be treated as cylindrical capacitors since they are concentrically arranged around the core leg. The calculation of these capacitances is as follows:

$$C = \frac{2\pi\epsilon_0\epsilon_r \cdot h}{\ln\left(\frac{d_2}{d_1}\right)} \quad (4)$$

where ϵ_0 is the permittivity of free space, ϵ_r is the relative permittivity of the dielectric, h is the height of the winding, and d_1 and d_2 are the inner and the outer diameters of the high- and low-

voltage windings. If the capacitance is between the winding and core, then d_1 is the inner diameter of the low-voltage winding and d_2 is the external diameter of the core leg.

In the case of shell-type transformers using interleaved windings with coils shaped as pancakes, (4) can be used to calculate the capacitance between windings and core. The parallel plate equation must be used to calculate the capacitances between windings (two pancakes) since the top and bottom sides of the windings are similar to parallel plates of a capacitor. For a complete description of the capacitances taken into account in three- and five-legged transformers, the methodologies used to calculate them refer to [21].

In cases where detailed design information is not available, calculation is not possible. Instead, the effective terminal capacitance can be measured with a capacitance bridge or determined based on the transient recovery voltage (TRV) oscillation frequency of each winding [15].

Capacitive effects are represented in the hybrid model with a capacitance matrix which, except for nodes α - β - γ , is a node-for-node overlay of the $[A]$ matrix, as shown in Fig. 5.

IV. CONCLUSION

A new hybrid transformer model for low and midfrequency transient simulations has been developed and presented, using strengths of both $[A]$ matrix and duality approaches, and also incorporating capacitive effects and the frequency dependency of resistances. Its application is aimed at low and midfrequency behaviors, such as excitation, inrush, switching transients, and ferroresonance.

The model is topologically correct, reflecting an actual core structure and including leakages between core and coils. The model represents the actual internal core and coil arrangements, and can be universally applied to delta, wye, auto, or zig-zag connections, which are made up as external jumper connections at the model's terminals.

V. FUTURE WORK

For future development, it is noted that $[A]$ and $[C]$ matrices can both be increased in size making it possible for higher-order L-C representation for higher frequencies. Thus, more detail for capacitive effects can be added, such as layer-to-layer or turn-to-turn capacitances. Modification of the $[A]$ and $[C]$ matrices will also allow simulation of internal faults.

APPENDIX TRANSFORMER PARAMETERS

Basic Ratings:

- three-legged stacked core transformer, 15-kVA, wye-delta dry-type transformer, 208Y/120:240;
- five-legged stacked core transformer, 150-kVA, grounded wye-wye oil-filled transformer, 12470GRY/7200:208Y/120.

Parameter	3-legged	5-legged
R_L, Ω	412.88	152.00
R_Y, Ω	312.74	105.77
R_4, Ω	291.38	10.353
L_4, mH	0.9716	4.140

Magnetization curves, three-legged transformer:

	$\lambda, \text{Wb-turn}$	i, A	
	Leg	0.0769	0.0891
0.1561		0.1011	
0.2352		0.1457	
0.3136		0.3008	
0.3901		0.7922	
0.4513		2.9316	
0.4565		4.0244	
0.4610		4.7901	
0.4667		5.4658	
0.4700	6.4886		
	$\lambda, \text{Wb-turn}$	i, A	
	Yoke	0.0769	0.5063
		0.1538	1.1295
		0.2311	1.9111
		0.3076	2.8818
		0.3811	4.2155
		0.4164	4.7608
		0.4228	5.3112
		0.4284	5.9544
		0.4348	6.2228
0.4400		7.2654	

Frequency-dependent Coil Resistance:

Parameter	3-legged	5-legged
High-voltage winding		
R_S, Ω	0.1412	3.9203
R_I, Ω	0.0102	443.54
L_I, mH	1830.0	22.633
R_2, Ω	0.2746	472.49
L_2, mH	0.0203	24.252
Low-voltage winding		
R_S, Ω	0.0313	0.0012
R_I, Ω	0.0021	0.1472
L_I, mH	698.44	0.0011
R_2, Ω	0.0476	0.0035
L_2, mH	0.0045	0.0006

Core:

Frequency-Dependent Coil Resistance:

Leakage Inductances Used to Build the $[A]$ -Matrix:

Capacitances Used to Build the $[C]$ -Matrix:

ACKNOWLEDGMENT

The modeling project is led by Michigan Technological University (MTU) in collaboration with North Dakota State University (NDSU). NDSU laboratory measurements have been useful

Magnetization curves, five-legged transformer:

	λ , Wb-turn	i , A
Leg	0.0754	0.1273
	0.1516	0.1300
	0.1894	0.1949
	0.2255	0.3022
	0.2450	0.3607
	0.2626	0.4672
	0.2813	0.5445
	0.3009	0.7394
	0.3192	1.0478
	0.3384	1.4800
	0.3575	2.0074
	0.3751	2.5694
Yoke	0.4134	4.2320
	0.4502	8.4298
	λ , Wb-turn	i , A
	0.2450	0.3055
	0.2626	0.3476
	0.2817	0.5964
	0.3009	0.8543
	0.3189	1.0770
	0.3384	1.3565
	0.3575	1.6892
	0.3751	2.1473
	0.4134	4.0842
0.4502	11.0414	

Leakage Inductances Used to Build the [A]-Matrix:

Parameter	3-legged	5-legged
X_{HL}, Ω	0.0640	31.5860
X_{HC}, Ω	0.1280	63.1720
X_{LC}, Ω	0.0448	22.1102

Capacitances Used to Build the [C]-Matrix:

Parameter	3-legged	5-legged
C_{H-T}, F	9.53E-09	2.545E-08
C_{X-T}, F	1.17E-08	6.000E-08
C_{HA-HB}, F	7.40E-09	1.158E-08
C_{HB-HC}, F	6.61E-09	1.158E-08
C_{HA-LA}, F	3.61E-08	3.56E-08
C_{HB-LB}, F	3.51E-08	3.64E-08
C_{HC-LC}, F	3.61E-08	3.56E-08

for model development, benchmarking, and parameter estimation.

REFERENCES

- [1] C. M. Arturi, "Transient simulation and analysis of a five-limb step-up transformer following an out-of-phase synchronization," *IEEE Trans. Power Del.*, vol. 6, no. 1, pp. 196–207, Jan. 1991.
- [2] T. Henriksen, "How to avoid unstable time domain responses caused by transformers models," *IEEE Trans. Power Del.*, vol. 17, no. 2, pp. 516–522, Apr. 2002.
- [3] P. Holenarsipur, N. Mohan, V. D. Albertson, and J. Christofersen, "Avoiding the use of negative inductances and resistances in modeling three-winding transformers for computer simulations," in *Proc. IEEE Power Eng. Soc. Winter Meeting*, Jan. 31–Feb. 4, 1999, vol. 2, pp. 1025–1030.

- [4] B. A. Mork, "Five-legged wound core transformer model: Derivation, parameters, implementation, and evaluation," *IEEE Trans. Power Del.*, vol. 14, no. 4, pp. 1519–1526, Oct. 1999.
- [5] D. L. Stuehm, B. A. Mork, and D. D. Mairs, "Five-legged core transformer equivalent circuit," *IEEE Trans. Power Del.*, vol. 4, no. 3, pp. 1786–1793, Jul. 1989.
- [6] D. L. Stuehm, Three-phase transformer core modeling—Final Rep. Bonneville Power Administration, Portland, OR, 1993, Award no. DE-B179-92BP26700.
- [7] Guidelines for Representation of Network Elements when Calculating Transients CIGRE Working Group 02 (SC 33), 1990.
- [8] H. W. Dommel, S. Bhattacharya, V. Brandwajn, H. K. Lauw, and L. Martí, *Electromagnetic Transients Program Reference Manual (EMTP Theory Book)*. Portland, OR: Bonneville Power, 1992.
- [9] Alternative Transients Program Rule Book. Heverlee, Belgium, K.U. Leuven EMTP Center, 1987.
- [10] H. K. Høidalen, B. A. Mork, D. Ishchenko, F. Gonzalez-Molina, and N. Chiesa, "Implementation of the hybrid transformer model in ATP-draw," in *Proc. Eur. EMTP-ATP Conf.*, Warsaw, Poland, 2005.
- [11] X. Chen, "Negative inductance and numerical instability of the saturable transformer component in EMTP," *IEEE Trans. Power Del.*, vol. 15, no. 4, pp. 1199–1204, Oct. 2000.
- [12] B. A. Mork and F. Gonzalez, Parameter estimation and advancements in transformer models for EMTP simulations. Task MTU-1: Develop prototype software interface & preprocessor Bonneville Power Administration, Portland, OR, 2002.
- [13] B. A. Mork, F. Gonzalez, and J. Mitra, Parameter estimation and advancements in transformer models for EMTP Simulations. Task MTU-4/NDSU-2: Develop Library of Model Topologies Bonneville Power, Portland, OR, 2003.
- [14] M. A. Bjorge, "Investigation of short-circuit models for a four-winding transformer," M.S. thesis, Dept. Elect. Eng., Michigan Tech. Univ., Houghton, 1996.
- [15] S. D. Cho, "Parameter estimation for transformer modeling," Ph.D. dissertation, Dept. Elect. Eng., Michigan Technological Univ., Houghton, 2002.
- [16] A. K. Sawhney, *A Course in Electrical Machine Design*. New York: Dhanpat Rai, 1994.
- [17] B. A. Mork, F. Gonzalez, and D. Ishchenko, "Leakage inductance model for autotransformer transient simulation," in *Proc. Int. Conf. Power System Transients*, Montreal, QC, Canada, 2005.
- [18] M. J. Gaffney, "Amorphous Core Transformer Model for Transient Simulation," M.S. thesis, Dept. Elect. Eng., Michigan Tech. Univ., Houghton, 1996.
- [19] D. C. Greyerbiehl, "Development and Investigation of an Anhyseretic Core Model," M.S., Dept. Elect. Eng., Michigan Tech. Univ., Houghton, MI, 1998.
- [20] D. C. Jiles and D. L. Atherton, *Theory of Ferromagnetic Hysteresis*. New York: Elsevier, 1986, vol. 61, pp. 48–60.
- [21] B. A. Mork, F. Gonzalez, and D. Ishchenko, Parameter estimation and advancements in transformer models for EMTP simulations. Task MTU-6: Parameter Estimation Bonneville Power, Portland, OR, 2003.
- [22] M. J. Heathcote, *The J&P Transformer Book*, 12th ed. New York: Newnes, 1998.
- [23] "CIGRE-Working Group 13.05, "The calculation of switching surges. II. Network representation for energization and re-energization studies on lines fed by an inductive source";" *Electra*, no. 32, pp. 17–42, 1974.
- [24] A. Schellmanns, J. P. Keradec, and J. L. Schannen, "Electrical equivalent circuit for frequency dependent impedance: Minimum lumped elements for a given precision," in *Proc. IEEE Industry Applications Conf.*, 2000, vol. 5, pp. 3105–3110.

Bruce A. Mork (M'82) was born in Bismarck, ND, on June 4, 1957. He received the B.S.M.E., M.S.E.E., and Ph.D. degrees in electrical engineering from North Dakota State University, Fargo, in 1979, 1981, and 1992, respectively.

From 1982 to 1986, he was a Design Engineer with Burns and McDonnell Engineering, Kansas City, MO, in the areas of substation design, protective relaying, and communications. He was in Norway for three years—as a Research Engineer for the Norwegian State Power Board, Oslo, from 1989 to 1990; as a Visiting Researcher with the Norwegian Institute of Technology, Trondheim, from 1990 to 1991; and as a Visiting Senior Scientist with SINTEF Energy Research, Trondheim, from 2001 to 2002. Currently, he is Associate Professor of Electrical Engineering and Director of the Power and Energy Research Center, Michigan Technological University, Houghton.

Dr. Mork is a member of the American Society for Engineering Education (ASEE), National Society of Professional Engineers (NSPE), and Sigma Xi. He is a registered Professional Engineer in the states of Missouri and North Dakota.

Francisco Gonzalez was born in Barcelona, Spain. He received the M.S. and Ph.D. degrees from the Universitat Politècnica de Catalunya, Barcelona, Spain, in 1996 and 2001, respectively.

As Visiting Researcher, he was with Michigan Technological University, Houghton; Tennessee Technological University, Memphis; North Dakota State University, Fargo; and at the Norwegian Institute of Science and Technology, Trondheim, Norway, where he was a Researcher involved in projects related to power. He was a Postdoctoral Student with Michigan Technological University. In 2005, he joined El Sewedy Cables, Cairo, Egypt. His research interests include transient analysis of power systems, lightning performance of transmission and distribution lines, flexible ac transmission systems (FACTS), power quality, and renewable energy.

Dr. Gonzalez is a member of the IEEE Power Engineering Society. In 2002, he received a Postdoctoral Fellowship from the Spanish Government.

Dmitry Ishchenko (M'04) was born in Krasnodar, Russia. He received the M.S. and Ph.D. degrees in electrical engineering from Kuban State Technological University, Krasnodar, in 1997 and 2002, respectively.

In 2000, he received the Norwegian Government Research Scholarship and worked as a Visiting Researcher with the Norwegian Institute of Science and Technology, Trondheim, Norway. His experience includes five years as Power Systems Engineer at the Southern Division of the Unified Energy System of Russia. In February 2003, he joined the Electrical and Computer Engineering Department, Michigan Technological University, Houghton, as a Postdoctoral Researcher. His research interests include computer modeling of power systems, power electronics, and power system protection.

Dr. Ishchenko is a member of the IEEE Power Engineering Society.

Don L. Stuehm (M'62) was born in Anamosa, IA, on February 5, 1941. He received the B.S. degree from Northrop University, Inglewood, CA, in 1962; the M.S. degree from North Dakota State University, Fargo, in 1967; and the Ph.D. degree from Colorado State University, Ft. Collins, in 1972.

From 1962 to 1965, he was with McDonnell-Douglas Corporation, St. Louis, MO, working on spacecraft systems. From 1965 to 1966, he was with Honeywell, Minneapolis, MN, working on control systems. From 1973 to 1976, he taught at the South Dakota School of Mines and Technology, Rapid City. In 1976, he joined the faculty of North Dakota State University, where he taught and conducted research in power systems. He is now Professor Emeritus.

Dr. Stuehm is a member of the IEEE Power Engineering Society, Eta Kappa Nu, Sigma Xi, and Phi Kappa Phi.

Joydeep Mitra (S'94–M'97–SM'02) received the B.Tech. (Hons.) degree in electrical engineering from the Indian Institute of Technology, Kharagpur, and the Ph.D. degree in electrical engineering from Texas A&M University, College Station.

Currently, he is Associate Professor of electrical engineering and Associate Director of the Electric Utility Management Program, New Mexico State University, Las Cruces. He was an Electrical Engineer for two years with Tata Steel, Jamshedpur, India; Senior Consulting Engineer with LCG Consulting, Los Altos, CA for three years; Assistant Professor with North Dakota State University, Fargo, for three years and two years with New Mexico State University. His research interests include power system reliability, distributed energy resources, and power system planning.